Journal of Thermal Analysis and Calorimetry (2020) 142:1457–1467
https://doi.org/10.1007/s10973-019-09144-1

Combustion analysis of biodiesel blends with different piston geometries

I. J. Isaac Premkumar[1] · A. Prabhu[2] · V. Vijayan[3] · A. Godwin Antony[3] · R. Venkatesh[4]

Received: 9 August 2019 / Accepted: 1 December 2019 / Published online: 20 December 2019

Abstract

Shallow reentrant piston (SRP) and deep cylindrical piston (DCP) geometries were designed by modifying the compression ratio of an engine with baseline hemispherical pistons. Three-dimensional (3D) models of the pistons were created using CREO software, and made with the help of erosion and electrochemical deposition techniques. The pressure variations in the SRP cylinder with rice bran, soya bean, and *Pongamia* methyl ester blends at 40% and 80% loading revealed 2–4% enhancements. The SRP shape demonstrated an improvement in the heat release rate (HRRs) for the blends with 4–8% biodiesel, which could result in longer ignition delays and a concentrated premixed combustion stage. Soya bean, rice bran, and *Pongamia* methyl ester blends exhibited lower HRRs for the DCP. Such modification of piston dimensions could be utilized to improve the engine efficiency with suitable biodiesel blends of *Pongamia* methyl esters. Overall, the results indicate that *Pongamia* biodiesel blends meet the requirements of engines with certain piston shapes to improve their performance while achieving complete combustion and high power. The results demonstrate that addition of biodiesel blends could achieve earlier combustion compared with diesel, which will support the oxidation stability of the fuel particles.

Keywords Compression ratio · Heat release rate · Biodiesel · Methyl ester blends · Oxidation stability

Introduction

Increasing the compression ratio (CR) from 16 to 18 can have various effects, including decreasing the brake-specific fuel consumption (BSFC) by about 30%, improving the brake thermal efficiency (BTE) by 13%, slightly decreasing the exhaust gas temperature, and decreasing the peak pressure by about 21%, 17%, and 10% at low, partial, and full load conditions, respectively, while also moving the high-pressure point towards top dead center (TDC) [1].

The minimum delay period is seen at full load at the most extreme CR value of 18, with a decrease of about 9% seen in the delay period, which expands in proportion to the pressure ratio at all loads [2]. The peak heat discharge occurs closer to TDC when the CR is increased from 16 to 18, while the maximum heat discharge is seen at higher loads. The most extreme pressure rise of 5.38 bar/crank angle degree (CAD) was obtained at CR of 18 and 100% load, and the maximum rate of pressure rise decreased when the CR was decreased, while the cumulative heat discharge was found to be higher for higher loads and pressure ratios. A pressure ratio of 18 is considered to be beneficial in terms of both better BTE and BSEC [3, 4].

✉ I. J. Isaac Premkumar
isaacpremkumar007@gmail.com

A. Prabhu
ashok.ct555@gmail.com

V. Vijayan
Vijayan.me@gmail.com

R. Venkatesh
venkidsec@gmail.com

[1] Mechanical Engineering Department, JCT College of Engineering and Technology, Coimbatore, Tamil Nadu, India

[2] Automobile Engineering Department, SRM University, Kattankulathur, Chennai, Tamil Nadu, India

[3] Mechanical Engineering Department, K. Ramakrishnan College of Technology, Tiruchirapalli, Tamil Nadu, India

[4] Mechanical Engineering Department, Kongunadu College of Engineering and Technology, Tiruchirapalli, Tamil Nadu, India

The impact of the cylinder bowl geometry on the combustion and discharge attributes of a diesel engine filled with biodiesel under medium-load condition has also been investigated. It was observed that the omega combustion cylinder (OCC) bowl geometry was more viable for achieving solid squeeze in a short time. Subsequently, the results for the OCC were found to be superior to those of a hemispherical combustion cylinder (HCC) or shallow-profundity combustion cylinder (SCC) at medium to high engine rates. Moreover, the production of CO was observed to be low as a direct result of the blend [5]. The impact of the swirl power and the turbulent force on the engine behavior has also been investigated, revealing that the use of a bowl with highly violent dynamics increases the capacity to achieve effective fuel interaction along with less whirl movement, which can be considered as an approach to improve engine operation. It has also been studied whether the use of methyl ester mixes can improve the performance of engines by introducing disturbance into the cylinder [6]. The twirl resulting from the grooves present on the cylinder head can enhanced the fuel–air interaction and help their mixing. Combined consideration of the impact of such altered combustion bowls and different biodiesel blend ratios is thus essential to identify biodiesel blends for use in compression ignition engines with cylinders showing enhanced turbulence and to establish proper compression ratios [7, 8].

The influence of the cylinder geometry and ignition structure on the operation of engines fueled by soya bean, rice bran, and *Pongamia* methyl esters at different mixes was studied in this work. Changing the pressure ratio of the engine, the cylinder geometry was adjusted from the standard hemispherical existing piston (HEP) to SRP or DCP, making it essential to explore the ignition properties of the various cylinder geometries and combustion chambers [9]. Different fuel blends with diesel content of 10%, 30%, and 50% were prepared and their impact on engine performance assessed at part and full load conditions using the different piston geometries. An ideal cylinder geometry for operation of the engine at high pressure ratio was found. Reasonable biodiesel mixes have been identified to achieve better engine operating attributes [10, 11].

The ecological effect of using alternate fuels blended with SiO_2 nanoadditives has also been presented. Use of corn oil methyl ester in emulsion form can significantly reduce CO, HC, CO_2, and NO_x emissions [19]. Algal fuel has also been shown to offer great improvements in terms of reducing the emission of particles during combustion. A similar approach based on introduction of zirconium oxide (ZrO_2) nanoadditives into *Azolla* algal oil biodiesel and *Spirulina* algal fuel has been applied. The properties of the fuels were tested to investigate their direct usability in compression ignition (CI) engines without modification [20, 22]. The results revealed that the CO, HC, and smoke emissions of the engine were inversely proportion to the amount of additives in the fuel. Natural vegetable oils have also been tested as substitutes for diesel fuel. Pine oil and linseed oil were added to diesel in an attempt to increase the performance of CI engines. The results of that work identified a successful combination of compression ratio, blend proportion, and operating load condition to achieve the application objectives [21, 23]. The aim of the work presented here is to reduce the emission of particles by diesel (CI) engines by applying various piston geometries and biodiesels. The main objective is to propose modified piston geometries to improve the combustion characteristics of such engines.

Materials and methods

Biodiesel preparation methods

Biodiesel was obtained using the transesterification technique by the reaction of oil with methanol under reflux conditions. Sodium hydroxide (NaOH, 0.5% v/v) and 1:3 by volume of methanol were added and worked up until the sodium hydroxide totally broke down in methanol, resulting in sodium methoxide [18]. *Pongamia* oil was added to the sodium methoxide by solid blending using a mechanical stirrer in the reactor. The temperature was kept at 65 °C for a reaction time of 1 h, then the blend was transferred to an isolating cup. The blend was allowed to settle for moderate time under gravity, yielding a clear brilliant fluid of unsaturated fat methyl esters with glycerol at the bottom. Biodiesel was obtained from rough rice bran by a transesterification procedure including the reaction of oil with methanol. Rice bran oil was introduced, and the reaction temperature was set at 65 °C. After reaction completion, the material was transferred to an isolating pipe and the two phases were isolated. The upper phrase was methyl ester (biodiesel), while the lower part was glycerin. Finally, rice bran methyl esters were collected. Biodiesel was obtained from rough soya bean oil by a transesterification process, including the reaction of oil with methanol [12]. Soya bean oil was added, and the reaction temperature was set at 60 °C for the test. After reaction termination, the material was transferred to an isolating pipe, and both phases were isolated. The upper phase was methyl ester (biodiesel), while the lower part was glycerin. The upper part consisting of soya bean biodiesel was collected.

Table 1 Physicochemical properties of oil blends

S. no.	Type of analysis	*Pongamia* oil blends			Soya bean oil blends			Rice bran oil blends		
		10%	30%	50%	10%	30%	50%	10%	30%	50%
1	Acidity, inorganic	Nil	Nil	Nil	Nil	Nil	Nil	Nil	Nil	Nil
2	Water content (KF titration)/ppm	447	428	410	475	463	433	450	427	417
3	Density at 15 °C in g cc^{-1}	0.802	0.811	0.821	0.806	0.81	0.823	0.81	0.812	0.821
4	Kinematic viscosity at 40 °C/mm^2 s^{-1}	1.98	2	2.12	2.8	2.12	2.18	2.17	2.12	2.2
5	Ash content	< 0.001%	< 0.001%	< 0.001%	< 0.001%	< 0.001%	< 0.001%	< 0.001%	< 0.001%	< 0.001%
6	Conradson carbon residue	< 0.01%	< 0.01%	< 0.01%	< 0.01%	< 0.01%	< 0.01%	< 0.01%	< 0.01%	< 0.01%
7	Flash point/°C	68	70	72	67	70	72	67	69	72
8	Copper strip corrosion at 100 °C in 3 h	Not worse than no. 1	Not worse than no. 1	Not worse than no. 1	Not worse than no. 1	Not worse than no. 1	Not worse than no. 1	Not worse than no. 1	Not worse than no. 1	Not worse than no. 1
9	Insoluble in hexane/%	0.00	0.00	0.00	0.00	0.00	0.00	0.00	0.00	0.00
10	Calculated cetane number	53	54	56	56	54	52	56	55	52
11	Heat of combustion/kJ kg^{-1}	41,535	41,365	40,265	41,570	40,945	39,940	41,235	40,525	39,495
12	Sulfur content/%	0.20	0.18	0.16	0.24	0.23	0.20	0.25	0.24	0.22

The obtained biodiesels were cleaned by expansion with 5% refining water to remove contamination from the blends. The methanolysis process gave 92% biodiesel [13].

Various biodiesel mixes including blends of 10%, 30%, and 50% of soya bean were obtained by expansion of diesel and biodiesel in the corresponding ratios:

1. B10: petroleum diesel (90%) + biodiesel (10%).
2. B30: petroleum diesel (70%) + biodiesel (30%).
3. B50: petroleum diesel (half) + biodiesel (half).

Comparable mixes at the same proportions were also obtained for rice bran and *Pongamia* biodiesels. The proportions in the biodiesels and their properties are presented in Table 1. The properties of the different B10, B30, and B50 biodiesels were assessed at ITA LAB, Chennai.

Experimental investigation

The experimental investigation was carried out using an electrical direct-current (DC) generator dynamometer test rig. The corresponding measurements are plotted at different functional loads. The discharge rate was determined using a Crypton gas analyzer. The cylinder pressure was determined utilizing a Kistler 701A transducer equipped with high-temperature links and cooling connector. The pressure transducer was utilized to quantify the cylinder pressure, heat discharge rate, and ignition delay over 50 progressive cycles. The values were normal and determined by enhancing the yield flag of the pressure transducer associated with information obtaining framework. The signal from the pressure transducer was enhanced through a charge amplifier then captured by a rapid data acquisition system [14]. The measurements were analyzed to obtain combustion parameters such as the start of the injection delay, maximum cylinder pressure, and HRR using a computer program. The HRR of the engine structure was determined using the condition in Eq. (1).

$$\frac{(\mathrm{d}Q_{\mathrm{ch}})}{\mathrm{d}t} = \frac{\gamma}{\gamma - 1} P \frac{\mathrm{d}V}{\mathrm{d}t} + \frac{1}{\gamma - 1} V \frac{\mathrm{d}P}{\mathrm{d}t}, \tag{1}$$

where γ is the ratio of the specific heat at constant pressure to that at constant volume, and $\mathrm{d}Q_{\mathrm{ch}}/\mathrm{d}t$ is the general HRR in kJ $^{\circ}\mathrm{C}^{-1}$ CA. The instantaneous P was estimated based on the pressure range, while V was defined based on the volume of the development system [15]. The test was performed using a water-cooled Kirloskar DM10-type single cylinder with pressure ratio of 16:1 as described in Table 2. The engine was placed on an AVL 20 eddy-current dynamometer. The air collection system was equipped with an orifice meter. The specific fuel consumption was determined using an AVL fuel meter and a PE10A fuel injection pump [16]. The crank angle position and pressure range were calculated and stored in the data acquisition system. A Crypton five-gas analyzer and Bosch smoke meter were applied to determine the amounts of CO, HC, NO_x, and smoke haziness, as shown in Fig. 1.

Piston geometric designs

The engine compression ratio was changed by altering the piston geometry. The molten wax technique was implemented to establish the different pressure ratios of the engine when using the pistons with different dimensions. Each piston was designed in SOLIDWORKS and converted to a 2D model. The HEP geometry bowl was adjusted to obtain the SRP and DCP designs. Adjustment of the piston bowl shape was applied to improve the quality of the air–fuel blend, the consumption rate, and the completeness of the ignition process [17]. The 2D profile of each cylinder is plotted in Fig. 2 to reveal the different dimensions of each piston design. The dimensions of the HEP geometry are presented in Table 3; comparable values were applied for the SRP and DCP designs, with the exception of the piston bowl measurements. The subtleties of the dimensional variety applied for each piston are discussed below in the corresponding setting.

Geometrical modeling

The different piston geometries were obtained in SOLIDWORKS software by using the three commands revolve, expel cut, and revolve cut in three directions [18].

The DCP, SRP, and HEP piston geometries were meshed using tetrahedral elements and corresponding nodes and elements, as shown in Fig. 3a–c. The basic properties of Al 7050 T7451 for the HEP were applied.

Modification of piston shape dimensions

The compression ratio of the engine was varied by adjusting the piston dimensions. The different piston geometries were constructed using erosion and electrochemical deposition techniques. The changes were implemented by furrowing away some metal from the cylinder bowl of the existing cylinder design. For the SRP design, approximately 4 mm was removed, close to the break in the current cylinder structure, whereas for the DCP geometry, 8 mm was removed close to the break in the current piston [4].

Table 2 Requirements for CI engine

Category of engine	Kirloskar DM10
Bore/mm	102
Stroke/mm	118
Fuel injection pressure/bar	190–200
Speed/rpm	1500
Compression ratio	16:1
Injection timing	26° BTDC
Capacity	984 cc
Maximum power	10 BHP
Fuel pump	PE10A
Injector nozzle type	P-type DSLA
Maximum needle lift/mm	0.2
Plunger diameter/mm	7
Maximum plunger stroke/mm	8
Prestroke/mm	4.3–4.5 with timer groove
Delivery valve/mm^3	21

Calculating the compression ratio

Wax was melted then poured into the cylinder and left for 30 min to determine the volume of the piston. The compression ratio of the HEP geometry was 16:1. The wax that had been poured inside the piston was then removed and warmed using an electric radiator. The liquid wax was poured into a 100-mL receptacle, and its volume noted. The quantity of wax for the SRP and DCP designs was found to be 19 mL and 26 mL, respectively, as shown in Fig. 4a–c.

Results and discussion

Effect on combustion pressure range for blends of soya bean, rice bran, and *Pongamia* biodiesels with HEP

The results demonstrated that, with the expansion of the biodiesel mixes, pre-ignition occurred, followed by diesel combustion, which will aid with complete oxidation of the

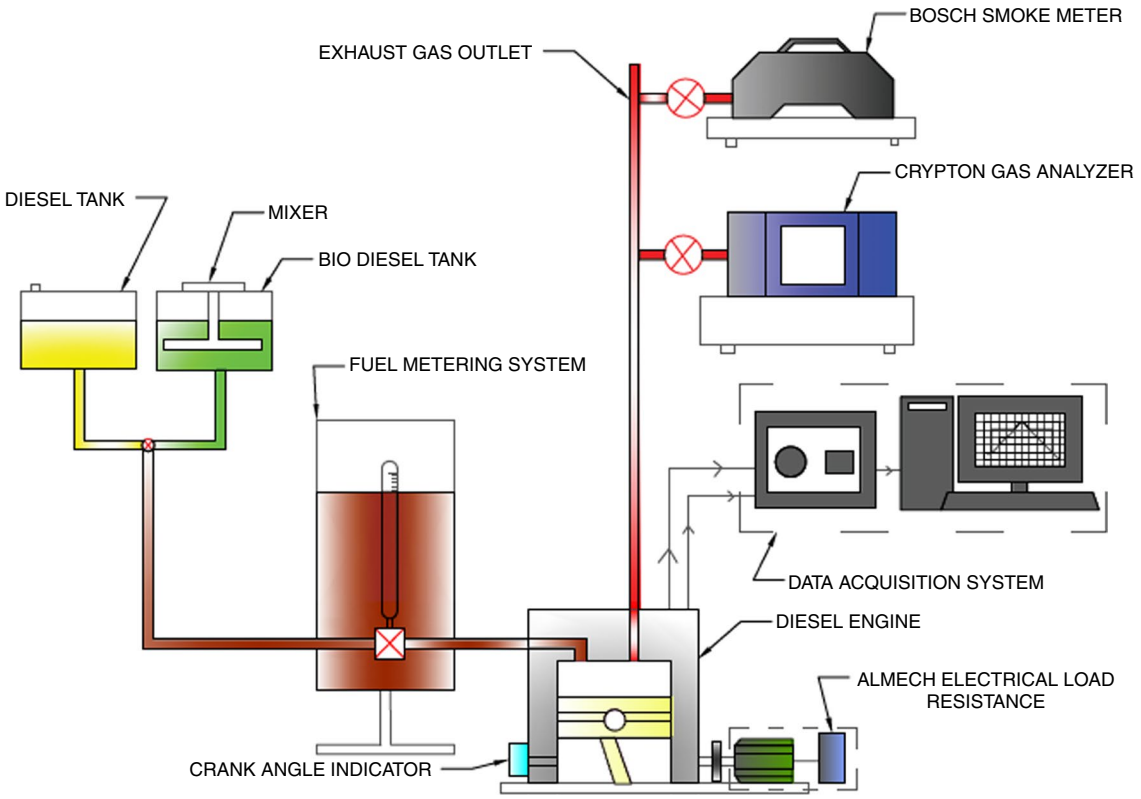

Fig. 1 Schematic diagram of experimental setup

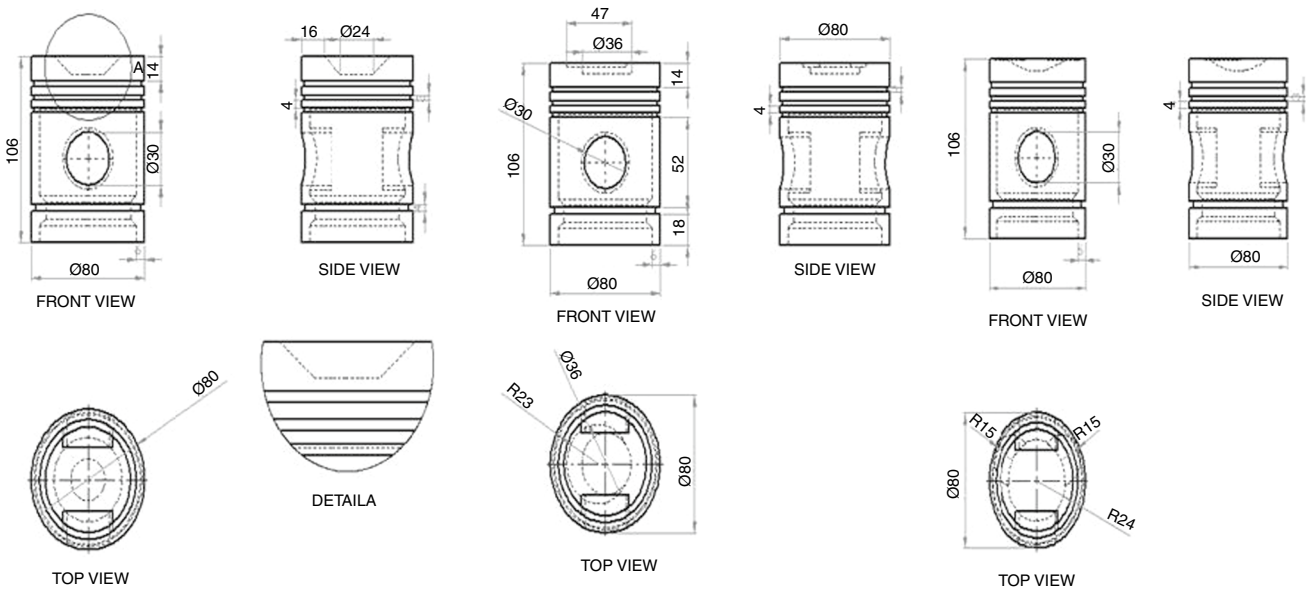

Fig. 2 Two-dimensional schematics of the DCP, SRP, and HEP geometries

Table 3 Specifications for hemispherical existing piston (HEP)

Piston dimension	Size in mm
Length of piston	106
Cylinder bore	80
Radial thickness of ring (t_1)	2
Axial thickness of ring (t_2)	3
Maximum thickness of cylinder (t_3)	6
Width of top land	14
Width of other ring land	4
Piston skirt	74

fuel particles. The premixed burning stage showed a quick pressure increase because of the improved start delay period that can be inferred from the improved thickness of the fuel in the methyl ester mixes.

Effect on combustion pressure range for blends of soya bean, rice bran, and *Pongamia* biodiesels with SRP

Figures 5–13 present the cylinder pressure range observed in the SRP, HEP, and DCP at the 80% load condition for the blends of soya bean, rice bran, and *Pongamia* methyl esters. Figures 5–7 show that the peak pressure in the HEP at 80% load state was 60 bar, 61 bar and 66 bar at 10%, 30% and 50% for soya bean, 65, 67, and 69 bar for rice bran at 10%, 30%, and 50%, and 59, 61, and 64 bar for *Pongamia* methyl ester blends at 10%, 30%, and 50%, respectively. Changing to the SRP geometry resulted in a 1–4% improvement in the pressure range, to 62, 63, and 65 bar for soya bean methyl esters, 65, 68, and 69 bar for rice bran methyl esters, and 68, 70, and 71 bar for *Pongamia* methyl esters, respectively, at the 80% load condition (Figs. 8–10).

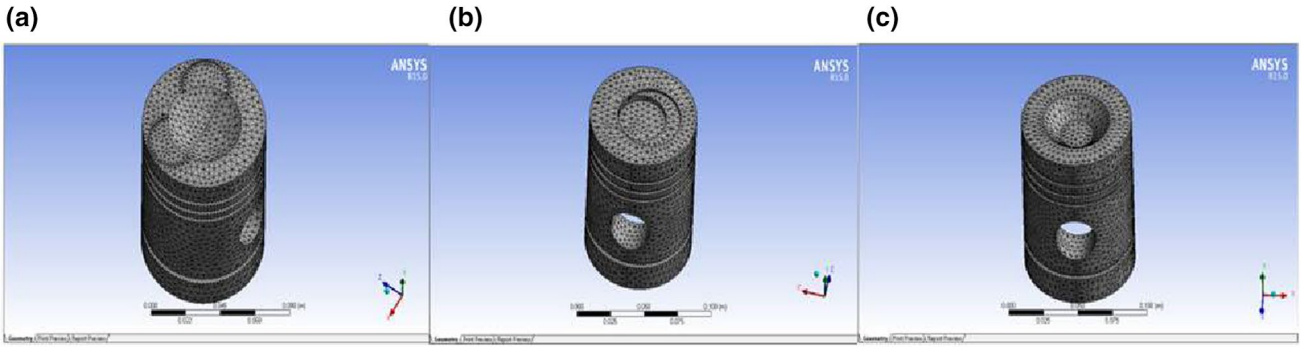

Fig. 3 **a**–**c** Meshes of the HEP, SRP, and DCP designs

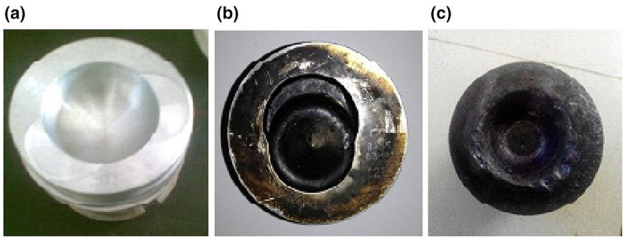

Fig. 4 **a** HEP, **c** SRP, and **c** DCP piston geometries

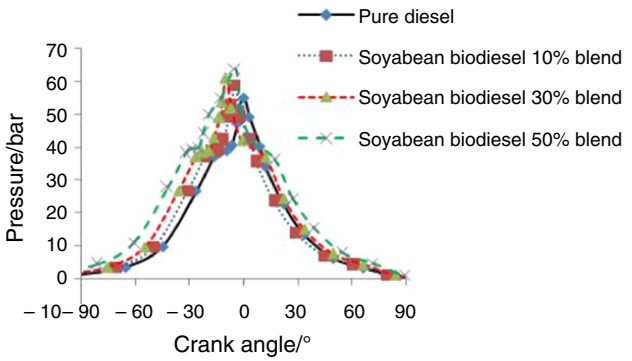

Fig. 5 Cylinder pressure at full load condition for blends of soya bean with HEP

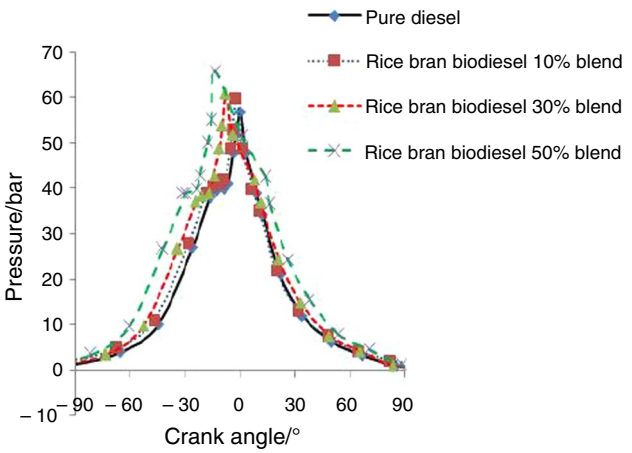

Fig. 6 Cylinder pressure at full load condition for blends of rice bran with HEP

Likewise, at the full load condition, these figures reveal that the cylinder pressure range for the diesel and methyl ester mixes of soybean, rice bran, and *Pongamia* was practically identical for the HEP and SRP, but decreased by 2–5% for the DCP. The cylinder pressure ranges for the soya bean, rice bran, and *Pongamia* methyl esters at 80% load with DCP are shown in Figs. 11–13, revealing a decrease of 2–6%,

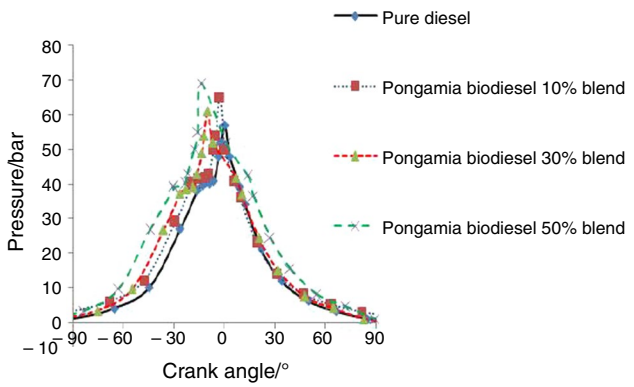

Fig. 7 Cylinder pressure at full load condition for blends of *Pongamia* with HEP

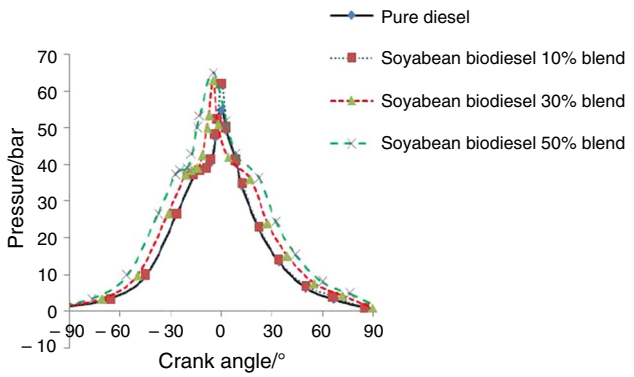

Fig. 8 Cylinder pressure at full load condition for blends of soya bean with SRP

potentially resulting from the shorter start delay and premixed burning period.

Effect on combustion heat release rate (HRR)

The effect on the heat release rate at 80% load for the soya bean, rice bran, and *Pongamia* methyl esters when using the HEP, SRP, and DCP shapes is shown in Figs. 14–22.

The signal acquired from the pressure transducer for each 0.26 CAD in 100 positions was used to compute the HRR, which is a critical parameter to investigate the combustion process and operating performance of engines. The results of the tests confirmed that, when using the HEP, the HRR was 1–4% higher for the biodiesel mixes in comparison with diesel, as shown in Figs. 14–16.

Changing to the SRP geometry resulted in enhancements of 4–8% in the HRR for the biodiesel mixes, which could be because of the longer start delay and more intense premixed burning stage as fuel was accumulated in the

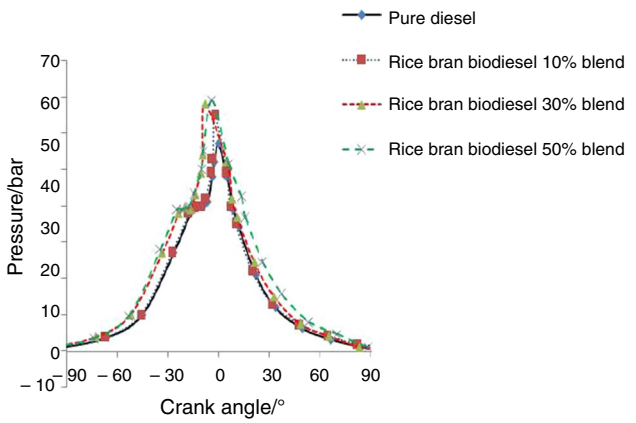

Fig. 9 Cylinder pressure at full load condition for blends of rice bran with SRP

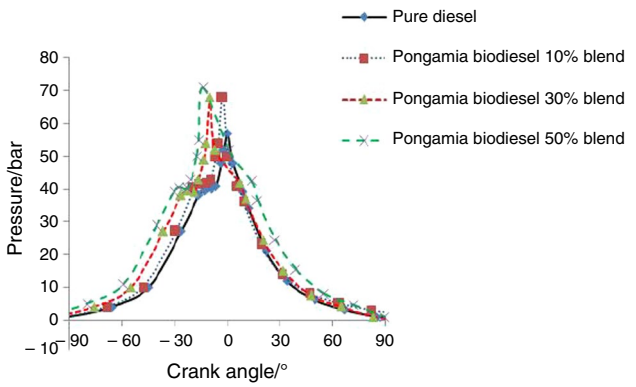

Fig. 10 Cylinder pressure at full load condition for blends of *Pongamia* with SRP

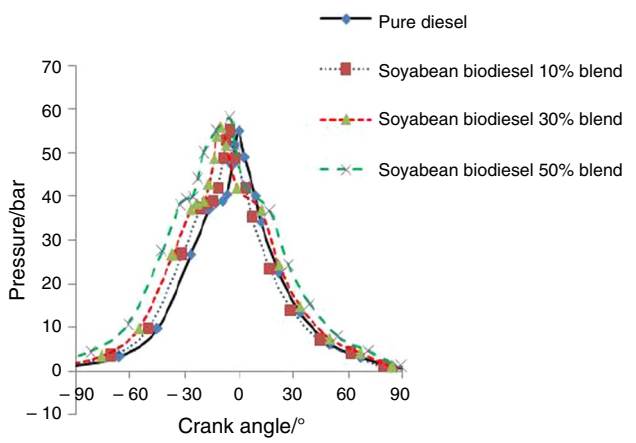

Fig. 11 Cylinder pressure at full load condition for blends of soya bean with DCP

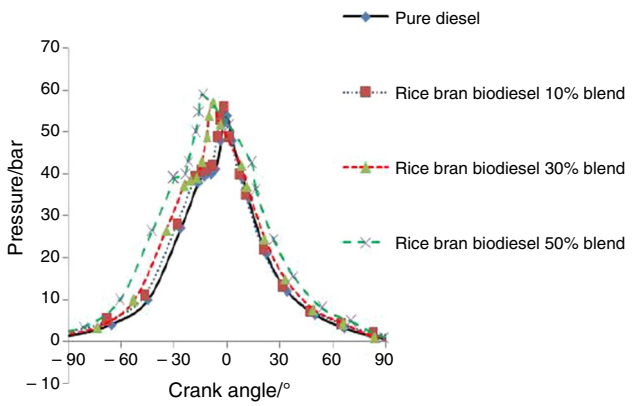

Fig. 12 Cylinder pressure at full load condition for blends of rice bran with DCP

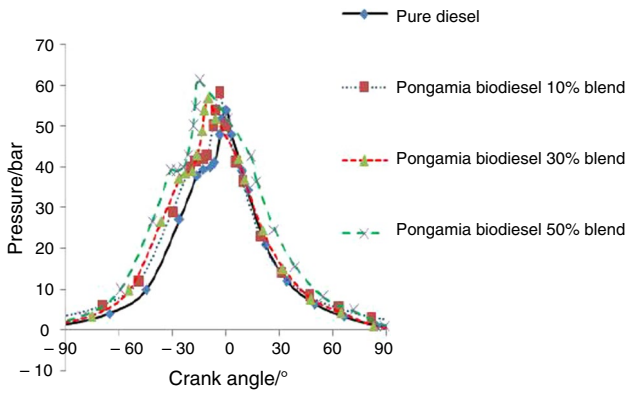

Fig. 13 Cylinder pressure at full load condition for blends of *Pongamia* with DCP

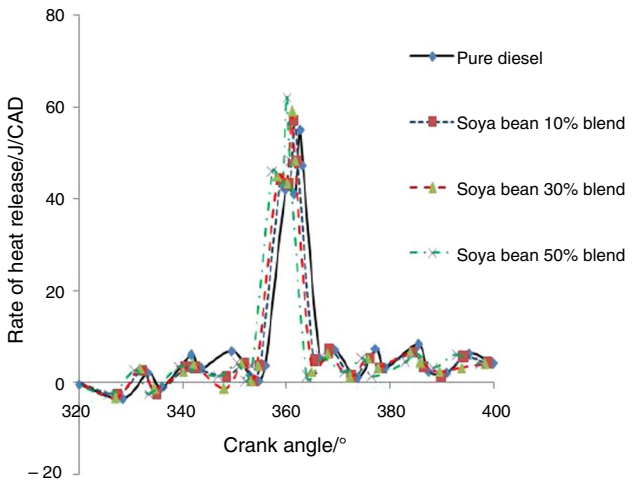

Fig. 14 HRR by combustion at 80% load for soya bean blends with HEP

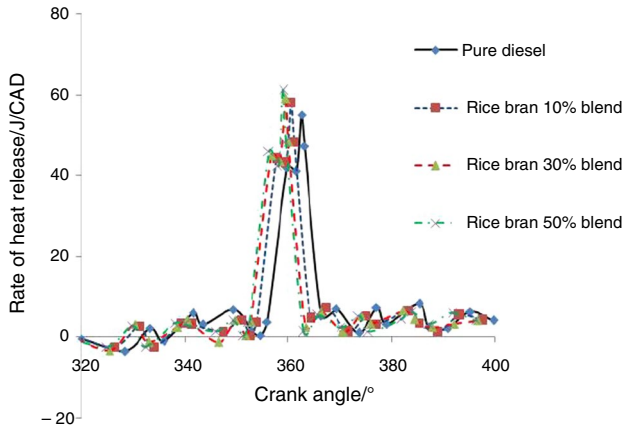

Fig. 15 HRR by combustion at 80% load for rice bran blends with HEP

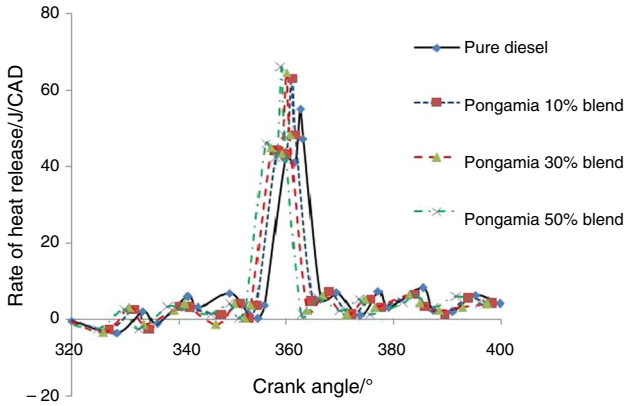

Fig. 16 HRR by combustion at 80% load for *Pongamia* blends with HEP

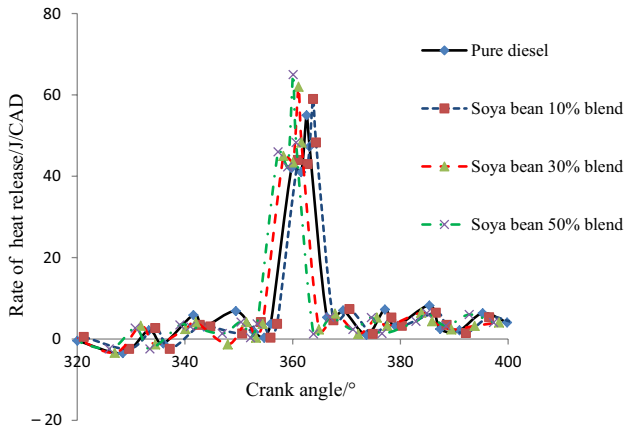

Fig. 17 HRR by combustion at 80% load for soya bean blends with SRP

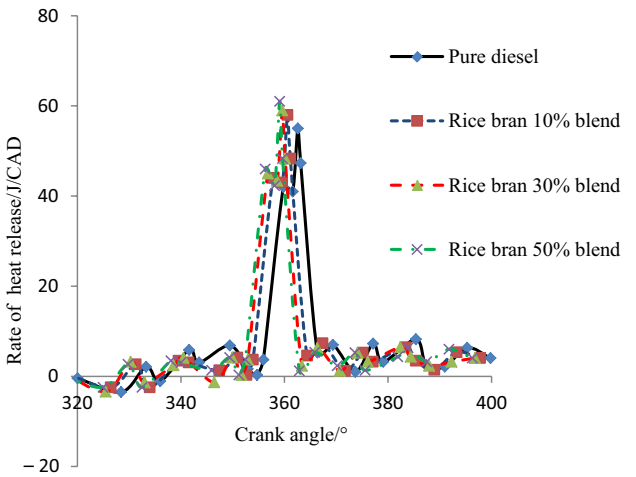

Fig. 18 HRR by combustion at 80% load for rice bran blends with SRP

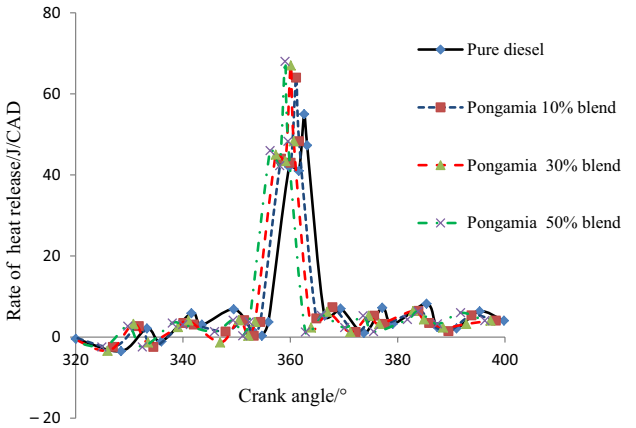

Fig. 19 HRR by combustion at 80% load for *Pongamia* blends with SRP

burning cylinder for a longer period and the time span of the whole combustion process was extended by increasing the start delay. Likewise, the HRR was higher for the *Pongamia* biodiesels for all the modified cylinder dimensions and loads, indicating that extra monoatomic oxygen was released throughout the combustion process after outright ignition began. The use of the mix of rice bran methyl esters likewise resulted in a 1–3% enhancement in the HRR, but this improvement was smaller when utilizing *Pongamia* methyl esters, as expected based on the lower calorific value and heat of vaporization. As the content of *Pongamia* methyl esters was increased, the HRR was additionally enhanced due to the more effecting blending of fuel with air and greater oxygen discharge at high loads. Similarly, use of the SRP design resulted in a 4–6% increase in the

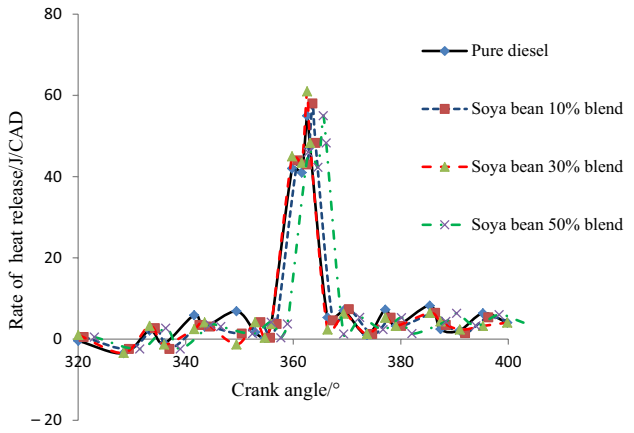

Fig. 20 HRR by combustion at 80% load for soya bean blends with DCP

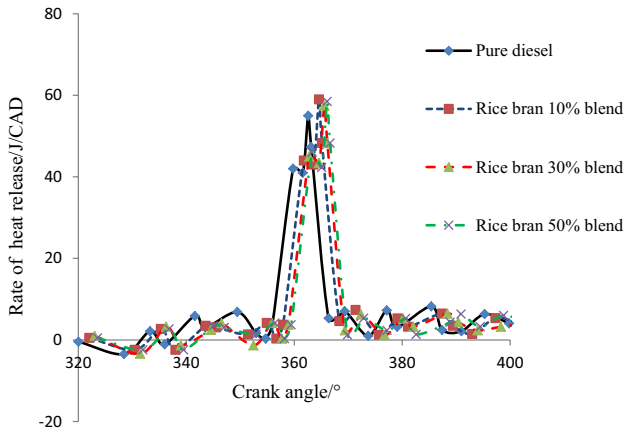

Fig. 21 HRR by combustion at 80% load for rice bran blends with DCP

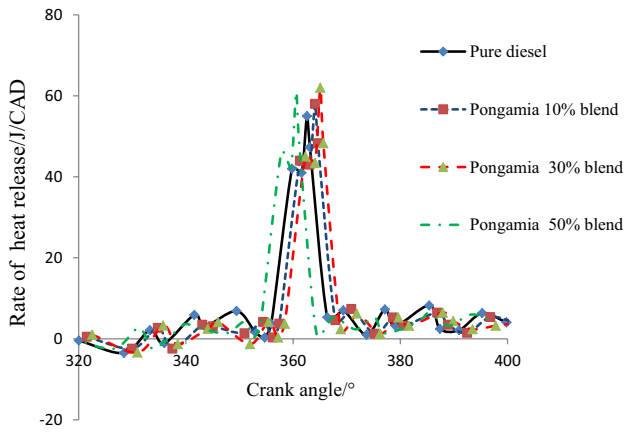

Fig. 22 HRR by combustion at 80% load for *Pongamia* blends with DCP

HRR in comparison with the HEP, which can be attributed to the longer start delay and greater amount of fuel available throughout this time for combustion, as demonstrated in Figs. 17–19. The results for the DCP with the soya bean, rice bran, and *Pongamia* methyl ester mixes are shown in Figs. 20 to 22, revealing a decline in the HRR for the HEP and SRP designs because of the generally shorter start delay and solid premixed ignition time.

Conclusions

The results obtained from the measurements on cylinders of different shapes can be summarized as follows: Combustion of *Pongamia*, rice bran, and soya bean esters was investigated in a single cylinder, and the effects of different cylinder dimensions on the pressure range and engine performance were measured. When using different biodiesel–diesel mixes, the engine operated well in all states. The combustion investigation revealed an increase in the maximum combustion pressure and heat release rate in all the studied conditions. The *Pongamia* oil methyl ester is thicker than diesel at low temperatures. Based on the differences between their properties, the combustion properties of the different biodiesel mixes also varied in all the studied conditions. The use of a piston with poor shape will result in ineffective air–fuel mixing. The 50% *Pongamia* mix resulted in a 2–7% enhancement in the pressure range at the 80% load state when using the SRP design. Mixes with higher content of soya bean, rice bran, and *Pongamia* methyl esters resulted in a 1–4% enhancement of the net HRR when using the SRP design.

Acknowledgements The authors acknowledge support from Dr. K. Lingadurai, Professor (Mechanical Engineering, University college of Engineering, Dindigul) and Dr. K. Raja, Associate Professor (Mechanical Engineering, University college of Engineering, Dindigul) for valuable scientific advice and support.

References

1. Li J, Yang WM, An H, Maghbouli A, Chou SK. Effects of piston bowl geometry on combustion and emission characteristics of biodiesel fueled diesel engines. Fuel. 2014;120:66–73.
2. Tamilvanan A, Balamurugan K, Vijayakumar M. Effects of nano-copper additive on performance, combustion and emission characteristics of *Calophyllum inophyllum* biodiesel in CI engine. J Therm Anal Calorim. 2015;136(1):317–30. https://doi.org/10.1007/s10973-018-7743-4.
3. Dahyabhai SV, Rathod PP. An experimental investigation on droplet ignition of bio-diesel and its blends. Int J Adv Eng Res Dev. 2014;1(5):1–15.
4. Hagos FY, Aziz AR, Sulaiman SA. Syngas (H_2/CO) in a spark-ignition direct-injection engine. Part 1: combustion, performance and emissions comparison with CNG. Int J Hydrogen Energy. 2014;39:17884–95.

5. Mohan Balaji, Yang Wenming, Chou Siawkiang. Fuel injection strategies for performance improvement and emissions reduction in compression ignition engines—a review. Renew Sustain Energy Rev. 2013;28:664–76.
6. Dantas MB, Albuquerque AR, Soledade LEB, Queiroz N, Maia AS, Santos IMG, Souza AL, Cavalcanti EHS, Barro AK, Souza AG. Biodiesel from soybean oil, castor oil and their blends—oxidative stability by PDSC and rancimat. J Therm Anal Calorim. 2011;106:607–11.
7. Saravankumar PT, Suresh V, Vijayan V, Godwin Antony A. Ecological effect of corn oil biofuel with SiO_2 nano additives. Energy Sources Part A: Recovery Util Environ Eff. 2019. https://doi.org/10.1080/15567036.2019.1576079.
8. Monyem Abdul, Van Gerpen Jon H. The effect of biodiesel oxidation on engine performance and emissions. Biomass Bioenerg. 2001;20:317–25.
9. Moser Bryan R, Williams Aaron, Haas Michael J, McCormick Robert L. Exhaust emissions and fuel properties of partially hydrogenated soybean oil methyl esters blended with ultra low sulfur diesel fuel. Fuel Process Technol. 2009;90:1122–8.
10. Cerit Muhammet. Thermo mechanical analysis of a partially ceramic coated piston used in an SI engine. Surf Coat Technol. 2011;205:3499–505.
11. Muneeswaran R, Thansekhar MR. Reduction of NO*x* emission in biodiesel (soyabean) fuelled DI diesel engine by cetane improver. ARPN J Eng Appl Sci. 2015;10(7):2968–73.
12. Jeevahan J, Mageshwaran G, Joseph GB, Raj RD, Kannan RT. Various strategies for reducing NOx emissions of biodiesel fuel used in conventional diesel engines: a review. Chem Eng Commun. 2014. https://doi.org/10.1080/00986445.2017.1353500.
13. Narayana Reddy J, Ramesh A. Parametric studies for improving the performance of a Jatropha oil-fuelled compression ignition engine. Renew Energy. 2006;31:1994–2016.
14. Nikanorova SP, Volkova MP, Gurina VN, Burenkova YU, Derkachenkoa LI, Kardasheva K, Regelb LL, Wilcoxb WR. Structural and mechanical properties of Al–Si alloys obtained by fast cooling of a levitated melt. Mater Sci Eng. 2005;390:63–9.
15. Nwafor O, Rice G, Ogbonna A. Effect of advanced injection timing on the performance of rapeseed oil in diesel engines. Renew Energy. 2000;21:433–44.
16. Pasupathy Venkateswaran S, Nagarajan G. Effects of the re-entrant bowl geometry on a DI turbocharged diesel engine performance and emissions—a CFD approach. J Eng Gas Turbines Power. 2010;132:1–10.
17. Pandian M, Sivapirakasam S, Udayakumar M. Investigation on the effect of injection system parameters on performance and emission characteristics of a twin cylinder compression ignition direct injection engine fuelled with Pongamia biodiesel–diesel blend using response surface methodology. Appl Energy. 2011;88:2663–76.
18. Park SH, Kim HJ, Lee CS. Effect of multiple injection strategies on combustion and emission characteristics in a diesel engine. Energy Fuels. 2016;30:810–8.
19. Saravankumar PT, Suresh V, Vijayan V, Godwin Antony A. Ecological effect of corn oil biofuel with SiO_2 nano-additives. Energy Sources Part A: Recov Util Environ Eff. 2019;41(23):2845–52.
20. Vijayan V, Sivachandran S, Saravanan S, Sivakumar V. Environmental effect of CI engine using microalgae biofuel with nano-additives. Energy Sources Part A: Recov Util Environ Eff. 2019;41(20):2429–38.
21. Antony AG, Dinesh S, Rajaguru K, Vijayan V, Aravind S. Analysis and optimization of performance parameters in computerized I.C. engine using diesel blended with linseed oil and Leishmaan's solution. Mech Mech Eng. 2017;21(2):193–205.
22. Govindasamy P, Godwin Antony A, Rajaguru K, Saravanan K. Experimental investigation of the effect of compression ratio in a direct injection diesel engine fueled with spirulina algae biodiesel. J Appl Fluid Mech. 2018;11:107–14.
23. Kishore Kumar J, Sundar Raj C, Sathishkumar P, Gopal P, Godwin Antony A. Investigation of performance and emission characteristics of diesel blends with pine oil. J Appl Fluid Mech. 2018;11:63–7.